

## Supporting Information

# Unraveling the charge transfer/electron transport in mesoporous TiO<sub>2</sub> films by voltabsorptometry

Christophe Renault,<sup>a</sup> Lionel Nicole,<sup>b</sup> Clément Sanchez,<sup>b</sup> Cyrille Costentin,<sup>a,\*</sup> Véronique Balland,<sup>a,\*</sup> and Benoît Limoges<sup>a,\*</sup>

<sup>a</sup>Laboratoire d'Electrochimie Moléculaire, UMR 7591 CNRS, Université Paris Diderot, Sorbonne Paris Cité, 15 rue Jean-Antoine de Baïf, F-75205 Paris Cedex 13, France.

<sup>b</sup>Laboratoire de Chimie de la Matière Condensée de Paris, UMR 7574 CNRS, UPMC-Paris 6-Collège de France, 11, place Marcelin Berthelot, 75231 Paris Cedex 05, France.

### Contents

1. Thermodynamic and kinetic data of mesoporous TiO<sub>2</sub> and SnO<sub>2</sub> films modified by redox-active functional molecules (Table S1).
2. Thin films characterization by SAXS and WACS experiments (Figure S1).
3. UV-visible absorption spectra and adsorption isotherms of Fe<sup>III</sup>TMPyP and Fe<sup>III</sup>-MP-11 adsorbed in a mesoporous EISA TiO<sub>2</sub> film (Figure S2).
4. UV-spectral changes recorded at a FeTMAPyP and MP-11-EISA TiO<sub>2</sub> electrode poised at different potentials (Figure S3).
5. Absorption changes as a function of time *t* recorded at a FeTMAPyP and MP-11-EISA TiO<sub>2</sub> electrodes (Figure S4 and S5).
6. Variation of the reduction peaks in DCVA as a function of the scan rate (Figures S6 and S7).
7. CV responses recorded at EISA TiO<sub>2</sub> electrodes different scan rates (Figure S8).
8. DCVAs of MP-11-loaded EISA TiO<sub>2</sub> electrodes at various scan rates (Figure S9).
9. Description of the general simple model of diffusion/charge transfer reaction in the film.
10. Formulation of the model in the framework of cyclic voltammetry and derivation of the current-potential relationships in the absence of adsorbed redox substrate.
11. Simulation of the charging current distorted by an ohmic drop.
12. Resolution in presence of an adsorbed redox couple in the case of fast electron diffusion in the framework of CV.

**1. Thermodynamic and kinetic data of mesoporous TiO<sub>2</sub> and SnO<sub>2</sub> films modified by redox-active functional molecules.**

**Table S1**

Molecule	Type of oxide film	MW (kDa)	<i>l</i> (nm)	$\gamma_{Fe^{III}}^{sat}$ (nmol cm <sup>-2</sup> )	$C_{Fe^{III}}^{sat}$ (mmol L <sup>-1</sup> )	$K_b$ ( $10^5$ M <sup>-1</sup> )	$k_{ads}$ (min <sup>-1</sup> )	Ref
Trianisylamine phosphonate	Nanocrystalline TiO <sub>2</sub> film	0.44	4800	208 <sup>b</sup>	720 <sup>b, c</sup>	0.26 <sup>d</sup>		S1
<sup>a</sup> cis-RuLL'-(NCS) <sub>2</sub>	Nanocrystalline TiO <sub>2</sub> film	0.88	5500	46 <sup>b</sup>	138 <sup>c</sup>			S2
			4000	154 <sup>b</sup>	640 <sup>b, c</sup>	0.12 <sup>d</sup>		S3
[Os(bpy) <sub>3</sub> (4,4'-(CO <sub>2</sub> H) <sub>2</sub> -bpy)] <sup>2+</sup>	Nanocrystalline TiO <sub>2</sub> film	1.04	4000	84 <sup>b</sup>	350 <sup>b</sup>	0.74 <sup>d</sup>		S4
[FeTMAPyP] <sup>5+</sup>	EISA TiO <sub>2</sub> film	0.91	220 ± 20	3	325 ± 100	1.4	Fast process: 0.62 min <sup>-1</sup>	This work
							Slow process: 0.012 min <sup>-1</sup>	
MP-11	EISA TiO <sub>2</sub> film	1.86	220 ± 20	3	230 ± 75	10	0.067 min <sup>-1</sup>	This work
Cyt-c	EISA TiO <sub>2</sub> film	12.4	240	0.41	43 ± 10	35	0.53 min <sup>-1</sup>	S5
Cyt-c	Nanocrystalline TiO <sub>2</sub> film	12.4	8000	19	40 <sup>b, c</sup>	1		S6
Flavodoxin	Nanocrystalline SnO <sub>2</sub> film	15-20	4000	4	15 <sup>b, c</sup>			S7
MP-11	Nanocrystalline SnO <sub>2</sub> film	1.86	4000	9	40 <sup>b, c</sup>			S8

<sup>a</sup> With L = 2,2'-bipyridyl-4,4'-dicarboxylic acid and L' = 4,4'-dinonyl-2,2'-bipyridyl.

<sup>b</sup> Recalculated from the data given in the work in reference.

<sup>c</sup> Considering an average film porosity of 60 vol%.

<sup>d</sup> Determined in MeOH or EtOH

S1. P. Bonhôte, E. Gogniat, S. Tingry, C. Barbé, N. Vlachopoulos, F. Lenzmann, P. Comte and M. Grätzel, *J. Phys. Chem. B*, 1998, **102**, 1498–507.

S2. Q. Wang, S. M. Zakeeruddin, M. K. Nazeeruddin, R. Humphry-Baker and M. Grätzel, *J. Am. Chem. Soc.*, 2006, **128**, 4446–52.

S3. X. Li, M. K. Nazeeruddin, M. Thelakkat, P. R. F. Barnes, R. Vilar and J. R. Durrant, *Phys. Chem. Chem. Phys.*, 2011, **13**, 1575–84.

S4. S. A. Trammell and T. J. Meyer, *J. Phys. Chem. B*, 1999, **103**, 104–7.

S5. C. Renault, V. Balland, E. Martinez-Ferrero, L. Nicole, C. Sanchez and B. Limoges, *Chem. Commun.*, 2009, 7494–6.

S6. E. Topoglidis, T. Lutz, R. L. Willis, C. J. Barnett, A. E. G.; Cass and J. R. Durrant, *Faraday Discuss.*, 2000, **116**, 35–46

S7. Y. Astuti, E. Topoglidis, P. B.; Briscoe, A. Fantuzzi, G. Gilardi and J. R. Durrant, *J. Am. Chem. Soc.*, 2004, **126**, 8001–9

S8. Y. Astuti, E. Topoglidis, G. Gilardi and J. R. Durrant, *Bioelectrochemistry*, 2004, **63**, 55–9.

**2. Thin films characterization by SAXS and WACS experiments.**

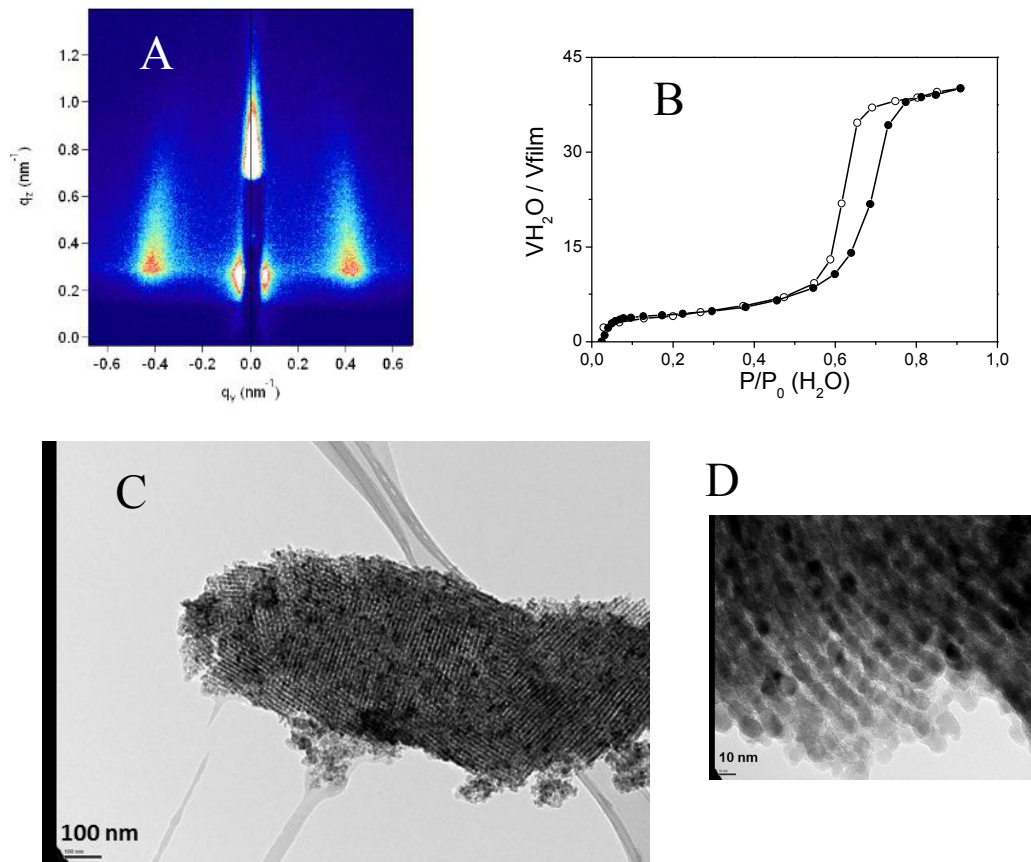


**Fig. S1.** (A) GI-SAXS pattern of  $\text{TiO}_2$  grid-like thin film. (B) Water Adsorption-desorption isotherm of  $\text{TiO}_2$  grid-like thin film. (C, D) TEM patterns of  $\text{TiO}_2$  grid-like thin film (anatase nanocrystals of about 7.5 nm).

**3. UV-visible absorption spectra and adsorption isotherms of Fe<sup>III</sup>TMPyP and Fe<sup>III</sup>-MP-11 adsorbed in a mesoporous EISA TiO<sub>2</sub> film.**

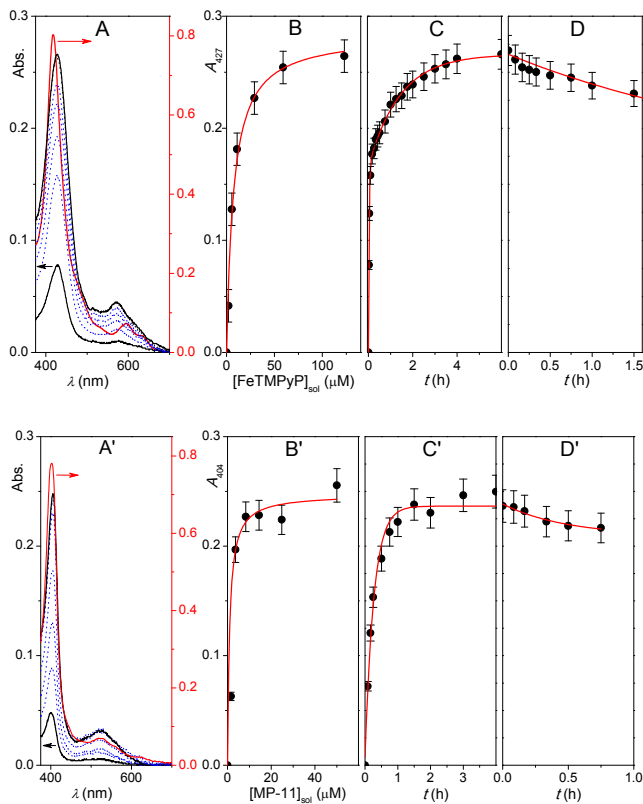


**Fig. S2.** UV-visible absorption spectra of (A) Fe<sup>III</sup>TMPyP and (A') Fe<sup>III</sup>-MP-11 adsorbed in a mesoporous EISA TiO<sub>2</sub> film ( $220 \pm 20$  nm-thick) on a ITO glass substrate. The spectra were recorded after the EISA TiO<sub>2</sub> film was immersed in a 50  $\mu\text{M}$  porphyrin solution (in 10 mM Hepes buffer, pH 7.0) for (from bottom to top) (A) 1, 5, 30, 60, 120, 240 min, one night, and (A') 2, 5, 10, 20, 30, 60, 75 min. Red lines: absorption spectrum of 8  $\mu\text{M}$  of (A) Fe<sup>III</sup>TMPyP and (A') Fe<sup>III</sup>-MP-11 in 10 mM Hepes buffer (pH 7.0, cell of 1-cm path length). Adsorption isotherms of (B) Fe<sup>III</sup>TMPyP and (B') Fe<sup>III</sup>-MP-11, including (red lines) fits to a Langmuir isotherm. Adsorption kinetics of (C) Fe<sup>III</sup>TMPyP and (C') MP-11 in a 50  $\mu\text{M}$  porphyrin, including (red lines) fits to a (C) double and (C') single exponential function. Desorption kinetics of (D) Fe<sup>III</sup>TMPyP and (D') MP-11 in a 200 mL Hepes buffer (10 mM, pH 7.0), including (red lines) fits to a simple exponential decay.

**Comments on the figure.** In contrast to the absorption spectrum of the immobilized MP-11, that is similar to the one in homogeneous solution, the spectrum of adsorbed Fe<sup>III</sup>TMPyP is slightly changed. The Q-band is blue shifted and the Soret band is somewhat red shifted as well as broadened as the concentration of adsorbed porphyrin is increased. This comportment suggests a surface binding effect on the heme coordination and perhaps some aggregation of porphyrin within the mesoporous structure.<sup>59</sup> The major driving force for the relatively strong adsorption of Fe<sup>III</sup>TMPyP in TiO<sub>2</sub> can be attributed to the electrostatic interactions between the positively charged porphyrin and the negatively charged TiO<sub>2</sub> interface at pH 7.0 ( $pI = 5.8$ )<sup>40</sup>. This is indirectly corroborated to the fact that the negatively charged [Fe<sup>III</sup>TPPS<sub>4</sub>]<sup>3-</sup> porphyrin (with TPPS<sub>4</sub> = tetrakis-4-sulfonatophenyl porphyrin) could not be adsorbed in TiO<sub>2</sub> films, except in the presence of a positively charged coadsorbent such as polylysine. Regardless of a low  $pI$  value of 4.8,<sup>48</sup> close to the one of TiO<sub>2</sub>, a significantly higher binding constant was determined for Fe<sup>III</sup>-MP-11, in line with that previously obtained for Fe<sup>III</sup>-Cyt-c in similar TiO<sub>2</sub> films.<sup>44</sup> The stronger affinity of MP-11 for TiO<sub>2</sub> is probably related to multiple noncovalent interactions

of the amino-acid residues with the metal oxide surface, including electrostatic, hydrogen bonds, van der Waals, and/or hydrophobic interactions.

The resistance of saturated  $\text{TiO}_2$  films to desorption is given by the change of maximal Soret band absorbance as a function of the soaking time in a heme-free buffer solution (plots D and D'). The desorption kinetics indicate that both of the modified electrodes are quite stable during prolonged immersion time in a heme-free buffer, leading to an only 10% desorption after 1 hour. This relatively good stability allows for their characterization by spectroelectrochemistry in a heme-free buffer solution.

#### 4. UV-spectral changes recorded at a FeTMPyP and MP-11-EISA $\text{TiO}_2$ electrodes poised at different potentials.

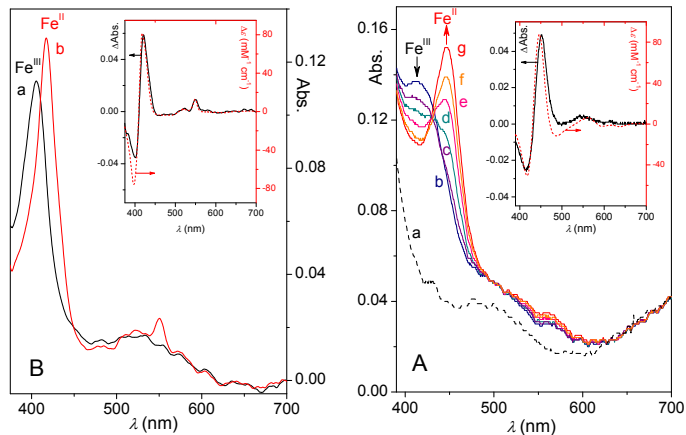


**Fig. S3.** (A) UV-spectral changes recorded at a FeTMPyP-EISA  $\text{TiO}_2$  electrode poised at different potentials: (b) +0.2 V to (c) 0, (d) -0.05, (e) -0.1, (f) -0.15, (g) -0.2 and (g) -0.4 V (vs. Ag/AgCl). (a) Blank spectrum recorded before adsorption of porphyrin. (B) UV-spectral changes (corrected from the blank spectrum) recorded at a MP-11-EISA  $\text{TiO}_2$  electrode held at: (a) +0.4 V and (b) -0.4 V (vs. Ag/AgCl). Insets: difference spectra between fully reduced and fully oxidized iron hemes in (plain black line) a EISA  $\text{TiO}_2$  film and (dotted red line) a homogeneous solution (on right scales are reported the difference extinction coefficients of the solution spectra).

**5. Absorption changes as a function of time recorded at a FeTMPyP and MP-11-EISA TiO<sub>2</sub> electrodes.**

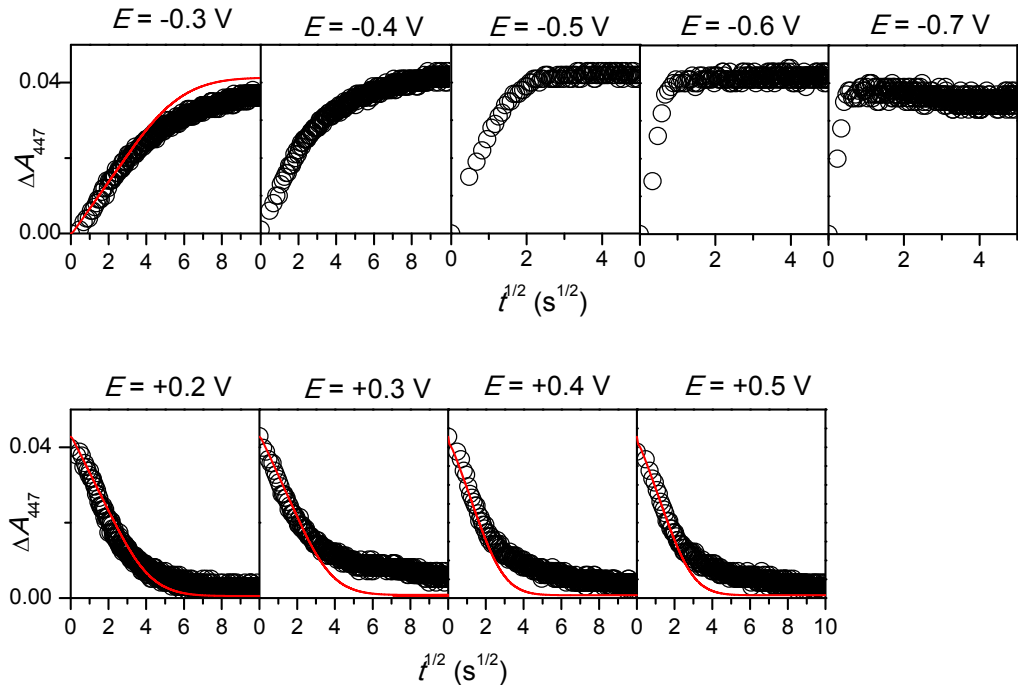


**Fig. S4.** Absorption changes as a function of  $\sqrt{t}$  recorded at a FeTMPyP-loaded EISA TiO<sub>2</sub> electrode ( $\gamma_{Fe^{III}} = 4.7 \times 10^{-10} \text{ mol/cm}^2$ ) after stepping the potential from (top row) +0.4 V or (bottom row) -0.6 V to the potential indicated on top of each graph. Red lines: fits of eq 2 to the experimental data.

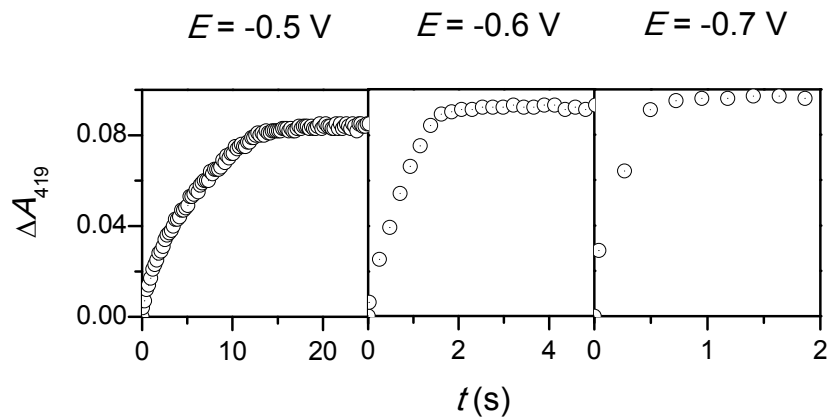


**Fig. S5.** Absorption changes as a function of time  $t$  recorded at a MP-11-loaded EISA TiO<sub>2</sub> electrode ( $\gamma_{MP-11} = 1.12 \times 10^{-9} \text{ mol/cm}^2$ ) after stepping the potential from +0.4 V to the potential indicated on top of each graph.

**6. Variation of the reduction peaks in DCVA as a function of the scan rate.**

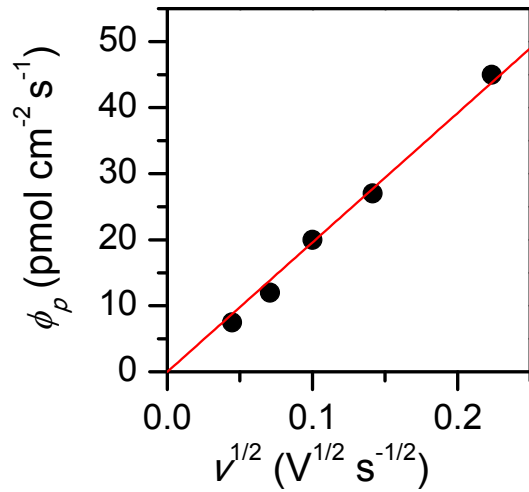


**Fig. S6.** Variation of the first reduction peak of FeTlMPyP in DCVA as a function of the square root of scan rate. Red line: linear regression. From the film concentration of FeTlMPyP (i.e. 32 mM) and the slope of the linear regression, an apparent film diffusion coefficient of  $D_O = 4.5 \times 10^{-12}$  cm<sup>2</sup> s<sup>-1</sup> can be calculated.

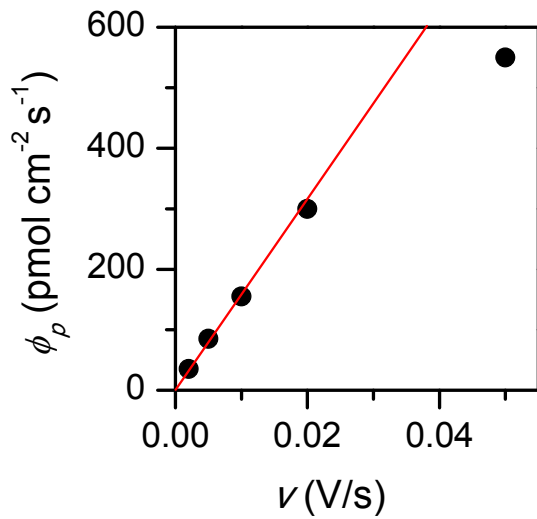


**Fig. S7.** Variation of the irreversible reduction peak of MP-11 in DCVA as a function of scan rate. Red line: linear fit to the slowest scan rates.

**7. CV responses recorded at EISA TiO<sub>2</sub> electrodes different scan rates.**

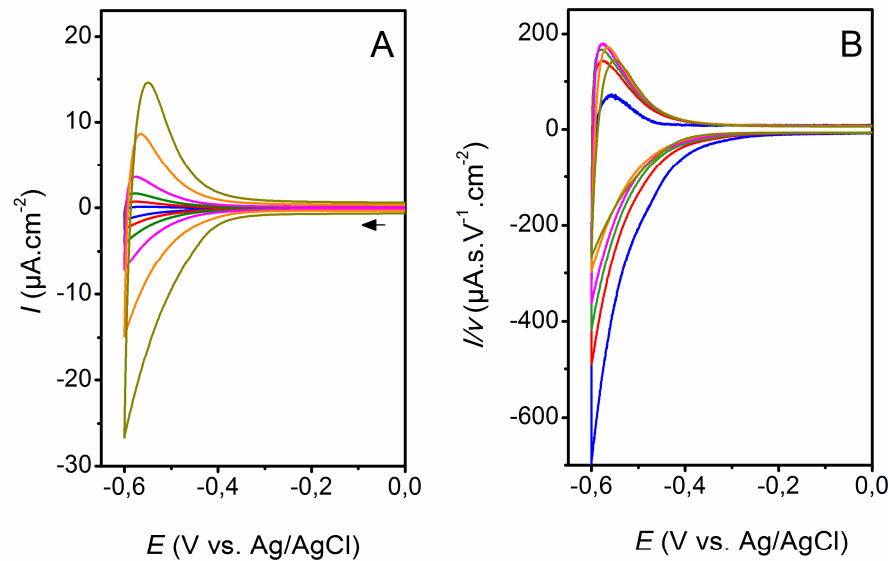


**Fig. S8.** CV responses recorded at EISA TiO<sub>2</sub> electrodes in Hepes buffer (10 mM) for different scan rate  $v$ : (blue) 2, (red) 5, (green) 10, (magenta) 20, (yellow) 50, (dark yellow) 100 mV/s. (A) Raw data. (B) Current density divided by the scan rate.

**8. DCVAs of MP-11-loaded EISA TiO<sub>2</sub> electrodes at various scan rates.**

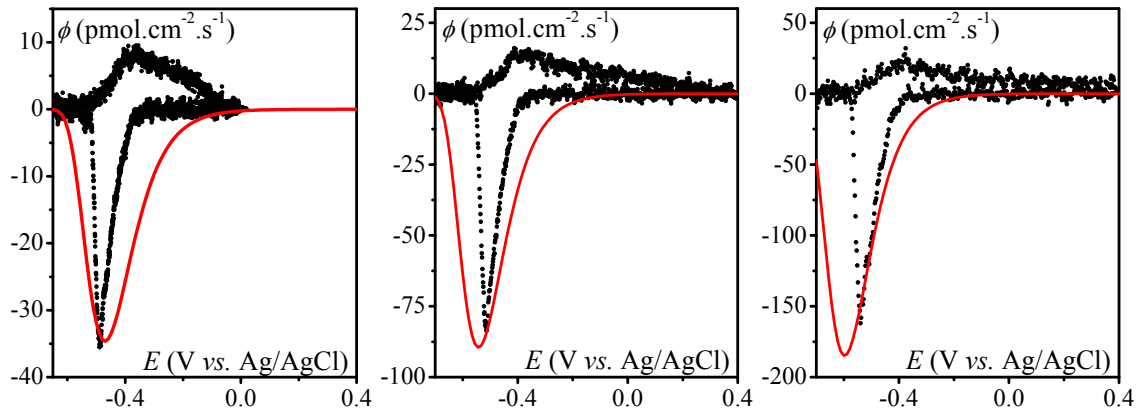


**Fig. S9.** Black dotted curves: DCVAs of MP-11-loaded EISA TiO<sub>2</sub> electrodes at various scan rates: (from left to right) 2, 5, and 10 mV s<sup>-1</sup>. Red curves: fits of eq 19 to the experimental plots using the following set of parameters:  $E_{CB} = -0.78$  V,  $kC_e^0 = 4$  s<sup>-1</sup>,  $\alpha = 0.32$  and from left to right  $\gamma_{Fe^{III}}^0 = 1.19, 1.23$ , and  $1.28$  nmol cm<sup>-2</sup>, respectively.

## 9. Description of the general simple model of diffusion/charge transfer reaction in the film

### 9.1. Description of the model

Oxidized substrate O is embedded in a semiconductive film of thickness  $d_f$ . Electrons are injected at the semiconductive film/ITO interface and the concentration of electrons at this interface is given by:

$$(C_e)_{x=0} = C_e^0 \exp\left[-\frac{F}{RT}(E - E_{CB})\right]$$

Once injected in the semiconductive film, electrons can diffuse (diffusion coefficient  $D_e$ ) and react with O (with a bimolecular rate constant  $k$ ) at the porous semiconductive/buffer interface giving the reduced product R. Although being adsorbed, O diffuse within the pores with a small diffusion coefficient D (but O and R cannot get out of the film). Moreover O can also be directly reduced into R (its diffusion coefficient is assumed to be equal to O diffusion coefficient) at the underlying conductive ITO surface (this interfacial electron transfer is described by a Butler-Volmer kinetics with a heterogeneous rate constant  $k^0$  and a transfer coefficient equal to 0.5).

### 9.2. General derivation of the model

In the film,  $0 < x < d_f$ :

$t > 0$ :

$$\frac{\partial C_e}{\partial t} = D_e \frac{\partial^2 C_e}{\partial x^2} - k C_O C_e$$

$$\frac{\partial C_O}{\partial t} = D \frac{\partial^2 C_O}{\partial x^2} - k C_O C_e$$

$$\frac{\partial C_R}{\partial t} = D \frac{\partial^2 C_R}{\partial x^2} + k C_O C_e$$

$$t = 0, C_e = 0, C_O = C_O^0, C_R = 0$$

In the solution,  $d_f < x$ :

$$C_e = 0, C_O = 0, C_R = 0$$

At the film/solution interface,  $x=d_f$ :

$$\left(\frac{\partial C_O}{\partial x}\right)_{x=d_f} = \left(\frac{\partial C_R}{\partial x}\right)_{x=d_f} = \left(\frac{\partial C_e}{\partial x}\right)_{x=d_f} = 0$$

At the conducting electrode surface,  $x=0$ :

$$(C_e)_{x=0} = C_e^0 \exp\left[-\frac{F}{RT}(E - E_{CB})\right]$$

$$\frac{I_{ph}}{F} = k^0 \exp\left[-\frac{F}{2RT}(E - E_{O/R}^0)\right] \left\{ (C_O)_{x=0} - (C_R)_{x=0} \exp\left[\frac{F}{RT}(E - E_{O/R}^0)\right] \right\} = D \left(\frac{\partial C_O}{\partial x}\right)_{x=0} = -D \left(\frac{\partial C_R}{\partial x}\right)_{x=0}$$

$$\frac{I_e}{F} = -D_e \left(\frac{\partial C_e}{\partial x}\right)_{x=0}$$

$$I = I_e + I_{ph}$$

corresponding to equations 5 to 7 in the text.

## 10. Formulation of the model in the framework of cyclic voltammetry and derivation of the current-potential relationships in the absence of adsorbed redox substrate.

### 10.1. Dimensionless formulation:

In the framework of cyclic voltammetry, the electrode potential is swept linearly from front to back between two values  $E_i$  and  $E_f$ :

$$0 \leq t \leq t_R : E = E_i - vt$$

$$t_R \leq t \leq 2t_R : E = E_f - v(t - t_R)$$

( $t_R$  is the time where the linear potential is reversed)

We define the normalized variables parameters so as to obtain a dimensionless formulation of the model:

$$\text{Time: } \tau = \frac{Fv}{RT} t$$

$$\text{Potential: } \xi = -\frac{F}{RT}(E - E_{CB}), \quad \xi' = -\frac{F}{RT}(E - E_{O/R}^0), \quad u_i = \frac{F}{RT}(E_i - E_{CB}), \quad u_f = \frac{F}{RT}(E_f - E_{CB}), \text{ in practice } u_i \gg 0 \text{ and } u_f \ll 0$$

$$\text{Space: } y = x \sqrt{\frac{Fv}{RTD}}$$

$$\text{Concentrations: } j = \frac{C_J}{C_O^0}, \text{ J being a species: } e, O, R$$

$$\text{Current: } \psi = \frac{I}{FC_O^0 \sqrt{D} \sqrt{\frac{Fv}{RT}}}$$

$$\text{Parameters: } \lambda = \frac{RT}{Fv} k C_O^0, \quad \gamma = \frac{C_e^0}{C_O^0}, \quad \delta = \frac{D_e}{D}, \quad l = \frac{d_f}{\sqrt{DRT/Fv}}, \quad l_e = \frac{d_f}{\sqrt{D_e RT/Fv}} = \frac{l}{\sqrt{\delta}}, \quad A = k^0 \sqrt{\frac{RT}{FvD}}$$

Using those parameters, the reaction-diffusion equations as well as the boundary conditions given in section 9 can be reformulated in dimensionless form:

In the film,  $0 < y < l$ :

$\tau > 0$ :

$$\frac{\partial e}{\partial \tau} = \delta \frac{\partial^2 e}{\partial y^2} - \lambda \times o \times e$$

$$\frac{\partial o}{\partial \tau} = \frac{\partial^2 o}{\partial y^2} - \lambda \times o \times e$$

$$\frac{\partial r}{\partial \tau} = \frac{\partial^2 r}{\partial y^2} - \lambda \times o \times e$$

$$\tau = 0, \quad e = 0, \quad o = 1, \quad r = 0$$

In the solution,  $l < y$ :

$$e = 0, \quad o = 0, \quad r = 0$$

At the film/solution interface,  $y = l$ :

$$\left( \frac{\partial o}{\partial y} \right)_{y=l} = \left( \frac{\partial r}{\partial y} \right)_{y=l} = \left( \frac{\partial e}{\partial y} \right)_{y=l} = 0$$

At the conducting electrode surface,  $y = 0$ :

$$(e)_{x=0} = \gamma \exp(\xi)$$

$$\psi_{ph} = \Lambda \exp(\xi'/2) \left[ (o)_{y=0} - (r)_{y=0} \exp(-\xi') \right] = \left( \frac{\partial o}{\partial y} \right)_{y=0} = - \left( \frac{\partial r}{\partial y} \right)_{y=0}$$

$$\psi_e = -\delta \left( \frac{\partial e}{\partial y} \right)_{y=0}$$

$$\psi = \psi_e + \psi_{ph}$$

### 10.2. Resolution in the absence of adsorbed redox substrate:

$\frac{\partial e}{\partial \tau} = \delta \frac{\partial^2 e}{\partial y^2}$ , transposed in the Laplace plane is:  $qe = \delta \frac{\partial^2 e}{\partial y^2}$  ( $q$  being the variable in the Laplace plane) leading to:

$$\bar{e} = \left[ (\bar{e})_{y=0} - \frac{1}{\sqrt{q/\delta}} \left( \frac{\partial \bar{e}}{\partial y} \right)_{y=0} \right] \frac{\exp(-\sqrt{q/\delta}y)}{2} + \left[ (\bar{e})_{y=0} + \frac{1}{\sqrt{q/\delta}} \left( \frac{\partial \bar{e}}{\partial y} \right)_{y=0} \right] \frac{\exp(-\sqrt{q/\delta}y)}{2}$$

$$\text{With: } \left( \frac{\partial \bar{e}}{\partial y} \right)_{y=l} = 0$$

Hence:

$$(\bar{e})_{y=0} = -\frac{\left( \frac{\partial \bar{e}}{\partial x} \right)_{y=0}}{\sqrt{\frac{q}{\delta}} \tanh\left(\sqrt{\frac{q}{\delta}}l\right)}$$

$$\text{with } \bar{\psi} = \bar{\psi}_e = -\delta \left( \frac{\partial \bar{e}}{\partial y} \right)_{y=0} \text{ because } \psi_f = 0$$

thus:  $(\bar{e})_{y=0} = \frac{\bar{\psi}}{\sqrt{q\delta} \tanh\left(\sqrt{\frac{q}{\delta}}l_e\right)} = \frac{\bar{\psi}}{\sqrt{q\delta} \tanh\left(\sqrt{ql_e}\right)}$ , i.e.  $(\bar{e})_{y=0} = \frac{\bar{\psi}'}{\sqrt{q} \tanh\left(\sqrt{ql_e}\right)}$  if we introduce  $\psi' = \psi / \sqrt{\delta}$ . The system is thus

$$\text{governed by only one parameter: } l_e = \frac{d_f}{\sqrt{D_e RT / Fv}}.$$

#### Limiting cases:

(i) When  $l_e = \frac{d_f}{\sqrt{D_e RT / Fv}} \rightarrow \infty$  (thick film or high scan rate or slow electron diffusion):

$(\bar{e})_{y=0} = \frac{\bar{\psi}'}{\sqrt{q}}$ , coming back in the real space we obtain an integral equation:  $\frac{1}{\sqrt{\pi}} \int_0^\tau \frac{\psi}{\sqrt{\tau-\eta}} d\eta = \gamma \exp(\xi)$ ; the CV is equivalent to the

foot-of-wave of a reversible one-electron Nernstian wave. The corresponding dimensional equation is:

$$\frac{1}{\sqrt{\pi}} \int_0^\tau \sqrt{\frac{RT}{Fv}} \frac{I_e}{\sqrt{t-\zeta}} d\zeta = F \sqrt{D_e} \sqrt{\frac{Fv}{RT}} C_e^0 \exp\left[-\frac{F}{RT}(E - E_{CB})\right]$$

The wave is not symmetrical and the current is proportional to  $\sqrt{v}$ .

(ii) When  $l_e = \frac{d_f}{\sqrt{D_e RT / Fv}} \rightarrow 0$  (thin film or low scan rate or fast electron diffusion):

$(\bar{e})_{y=0} = \frac{\bar{\psi}'}{ql_e}$ , coming back in the real space:  $\int_0^\tau \frac{\psi'}{l_e} d\eta = \gamma \exp(\xi)$ , ie.:  $\psi' = l_e \gamma \exp(\xi)$  in the forward scan and  $\psi' = -l_e \gamma \exp(\xi)$  in

the reverse scan. The wave is symmetrical and the current is proportional to  $v$ . The corresponding dimensional equation is:

$$I_e = \pm \frac{F^2 v}{RT} d_f C_e^0 \exp\left[-\frac{F}{RT}(E - E_{CB})\right].$$

## 11. Simulation of the charging current distorted by an ohmic drop.

In the presence of a series resistance,  $R_s$ , the true potential witnessed by TiO<sub>2</sub> while cycling the potential between starting ( $E_i$ ) and final potentials ( $E_f$ ) is expressed in the cathodic direction by

$$E = E_i - vt - R_s i_C$$

and in the anodic one by

$$E = E_f + vt - R_s i_C$$

while the capacitive current density  $I_C$  passing through the cell is described by:

$$I_C = \frac{i_C}{S} = \frac{dQ}{Sdt} = \frac{dQ}{SdE} \frac{dE}{dt} = C \frac{dE}{dt}$$

With  $C = C_{ch} + C_{ITO}$  where  $C_{ch}$  is given by eq 19 (see text).

Therefore, for an exponential capacitance with a series resistance, we have

$$\frac{dE}{du} = \frac{E_i - v\tau u - E}{\exp\left(-\alpha \frac{F}{RT} E\right) + \frac{C_{ITO}}{C_t}}$$

for the forward cathodic scan, and

$$\frac{dE}{du} = \frac{E_f + v\tau u - E}{\exp\left(-\alpha \frac{F}{RT} E\right) + \frac{C_{ITO}}{C_t}}$$

for the backward anodic one. Here,  $C_t = C_{trap,0} \exp(\alpha E_{CB} F/RT)$ ,  $u = t/\tau$  and  $\tau = R_s C_t S$ .

The equations can be solved numerically using the fourth order Runge-Kutta method. Once  $E$  is known, the current could be easily determined and the CV plot then simulated.

## 12. Resolution in presence of an adsorbed redox couple in the case of fast electron diffusion in the framework of CV.

In such a situation, the total current is the sum of a faradaic component (here noted  $\psi_f$ , which is itself the sum of two terms, see below) and an apparent capacitive component  $\psi_c$ , corresponding to the injection of the electrons in the TiO<sub>2</sub> matrix establishing the uniform concentration of electron and allowing the faradaic component noted  $\psi_f$  below to take place. As shown in section 10 of this SI,  $\psi_c = \pm I_e \gamma \sqrt{\delta} \exp(\xi)$ , corresponding thus to the background current. The advantage of spectroelectrochemistry is to permit to visualize only the faradaic component, that is the reason why we only derive below equations to get  $\psi_f$ .

The system to be solved is –in the dimensionless formulation):

In the film,  $0 < y < l$ :

$\tau > 0$ :

$$e = \gamma \exp(\xi)$$

$$\frac{\partial o}{\partial \tau} = \frac{\partial^2 o}{\partial y^2} - \lambda \times o \times e$$

$$\frac{\partial r}{\partial \tau} = \frac{\partial^2 r}{\partial y^2} - \lambda \times o \times e$$

$$\tau = 0, e = 0, o = 1, r = 0$$

In the solution,  $l < y$ :

$$e = 0, o = 1, r = 0$$

At the film/solution interface,  $y = l$ :

$$\left( \frac{\partial o}{\partial y} \right)_{y=l} = \left( \frac{\partial r}{\partial y} \right)_{y=l} = 0$$

At the conducting electrode surface,  $y = 0$ :

$$\psi_{f,1} = \lambda \int_0^l e \times o dy$$

$$\psi_{f,2} = \Lambda \exp(\xi'/2) \left[ (o)_{y=0} - (r)_{y=0} \exp(-\xi') \right] = \left( \frac{\partial o}{\partial y} \right)_{y=0} = - \left( \frac{\partial r}{\partial y} \right)_{y=0}$$

$$\psi_f = \psi_{f,1} + \psi_{f,2}$$

We consider the case in which  $E_{O/R}^0 \gg E_{CB}$ :

At high enough potential (i.e.  $\xi \rightarrow -\infty$ ), we can consider that  $e = \gamma \exp(\xi) \rightarrow 0$  and thus  $\psi_{f,1} \rightarrow 0$ . We are thus lead to the following equations:

In the film,  $0 < y < l$ :

$\tau > 0$ :

$$\frac{\partial o}{\partial \tau} = \frac{\partial^2 o}{\partial y^2}$$

$$\frac{\partial r}{\partial \tau} = \frac{\partial^2 r}{\partial y^2}$$

$$\tau = 0, e = 0, o = 1, r = 0$$

In the solution,  $l < y$ :

$$o = 0, r = 0$$

At the film/solution interface,  $y = l$ :

$$\left(\frac{\partial o}{\partial y}\right)_{y=l} = \left(\frac{\partial r}{\partial y}\right)_{y=l} = 0$$

At the conducting electrode surface,  $y = 0$ :

$$\psi_f = \psi_{f,2} = \Lambda \exp(\xi'/2) \left[ (o)_{y=0} - (r)_{y=0} \exp(-\xi') \right] = \left(\frac{\partial o}{\partial y}\right)_{y=0} = -\left(\frac{\partial r}{\partial y}\right)_{y=0}$$

This set of equations is exactly the one corresponding to a reversible one electron wave in a thin film with slow electron transfer. The

wave is governed by two parameters  $l = \frac{d_f}{\sqrt{DRT/Fv}}$  and  $\Lambda = k^0 \sqrt{\frac{RT}{FvD}}$ . At low scan rate a reversible adsorption wave is expected

whereas a diffusive slow electron transfer is expected.

At low enough potential (i.e.  $\xi' \rightarrow \infty$ ), we can consider that  $\psi_{f,2} \rightarrow 0$  and  $\psi_f = \psi_{f,1}$ . The system is then governed by two parameters

$l = \frac{d_f}{\sqrt{DRT/Fv}}$  and  $\lambda\gamma = \frac{RT}{Fv} kC_e^0$ . It is not possible to get an analytical equation for  $\psi_{f,1}$  in the general case but if we consider

the limiting case where space zone in which there is a depletion of O due to the first wave is small,  $l \rightarrow \infty$ .

Then, in the film  $0 < y < l$ :

$$e = \gamma \exp(\xi)$$

$$\frac{\partial o}{\partial \tau} \approx -\lambda \times o \times e \text{ leading to: } o = \exp\left(-\int_0^\tau \lambda \times e \, d\eta\right)$$

Finally:

$$\psi_f = \psi_{f,1} = \lambda\gamma l \exp(\xi) \exp[-\lambda\gamma \exp(\xi)]$$

If we define  $\psi'' = \psi/l$  and  $\xi'' = \xi + \ln(\lambda\gamma)$  then  $\psi'' = \exp(\xi'') \exp(-\exp(\xi''))$  corresponding to:

$$\phi_f = \frac{I_f}{F} = \frac{I_{f,1}}{F} = kC_e^0 C_o^0 d_f \exp\left[-\frac{F}{RT}(E - E_{CB})\right] \exp\left\{-\frac{RT}{Fv} kC_e^0 \exp\left[-\frac{F}{RT}(E - E_{CB})\right]\right\} \text{ (equation 12 in the text).}$$

In case where the interfacial electron transfer with O is exclusively governed by the electrons trapped in the localized states of the semiconductor, the term  $e = \gamma \exp(\xi)$  has to be replaced by the following one:

$$e = \gamma \exp(\alpha\xi)$$

where the parameter  $\alpha$  reflects the distribution of traps in the bandgap of the semiconductor. Under these conditions, the above limiting case leads to an alternative expression of  $\psi_f$ :

$$\psi_f = \psi_{f,1} = \lambda\gamma l \exp(\alpha\xi) \exp[-\lambda\gamma \exp(\alpha\xi)] \text{ corresponding to:}$$

$$\phi_f = \frac{I_f}{F} = \frac{I_{f,1}}{F} = kC_e^0 C_o^0 d_f \exp\left[-\alpha \frac{F}{RT}(E - E_{CB})\right] \exp\left\{-\frac{RT}{Fv} kC_e^0 \exp\left[-\alpha \frac{F}{RT}(E - E_{CB})\right]\right\} \text{ (equation 15 in the text).}$$